



RESEARCH LETTER

10.1029/2021GL097246

Rapid Acidification of the Arctic Chukchi Sea Waters Driven by Anthropogenic Forcing and Biological Carbon Recycling

Di Qi^{1,2,3} , Yingxu Wu^{1,2} , Liqi Chen^{1,2} , Wei-Jun Cai⁴ , Zhongxian Ouyang⁴ , Yixing Zhang², Leif G. Anderson⁵ , Richard A. Feely⁶, Yanpei Zhuang¹, Hongmei Lin², Ruibo Lei⁷ , and Haibo Bi³

¹Polar and Marine Research Institute, College of Harbor and Coastal Engineering, Jimei University, Xiamen, China, ²Third Institute of Oceanography, MNR, Xiamen, China, ³Center for Ocean Mega-Science, Chinese Academy of Sciences, Qingdao, China, ⁴School of Marine Science and Policy, University of Delaware, Newark, DE, USA, ⁵Department of Marine Sciences, University of Gothenburg, Gothenburg, Sweden, ⁶Pacific Marine Environmental Laboratory/NOAA, Seattle, WA, USA, ⁷Key Laboratory for Polar Science of the MNR, Polar Research Institute of China, Shanghai, China

Key Points:

- pH and Ω_{arag} declined at $-0.0047 \pm 0.0026 \text{ years}^{-1}$ and $-0.017 \pm 0.009 \text{ years}^{-1}$ from 2002 to 2019, 2–3 times greater than atmospheric CO_2 projected
- The enhanced acidification in Chukchi Sea is mainly driven by enhanced dissolved inorganic carbon, owing to atmospheric CO_2 uptake and biological activity
- Aragonite undersaturation in Pacific Winter Water has been observed from 2010; other water masses are expected to encounter $\Omega_{\text{arag}} < 1$ within 15 years

Supporting Information:

Supporting Information may be found in the online version of this article.

Correspondence to:

D. Qi,
qidi60@qq.com

Citation:

Qi, D., Wu, Y., Chen, L., Cai, W.-J., Ouyang, Z., Zhang, Y., et al. (2022). Rapid acidification of the Arctic Chukchi Sea waters driven by anthropogenic forcing and biological carbon recycling. *Geophysical Research Letters*, 49, e2021GL097246. <https://doi.org/10.1029/2021GL097246>

Received 30 NOV 2021
Accepted 28 JAN 2022

Abstract The acidification of coastal waters is distinguished from the open ocean because of much stronger synergistic effects between anthropogenic forcing and local biogeochemical processes. However, ocean acidification research is still rather limited in polar coastal oceans. Here, we present a 17-year (2002–2019) observational data set in the Chukchi Sea to determine the long-term changes in pH and aragonite saturation state (Ω_{arag}). We found that pH and Ω_{arag} declined in different water masses with average rates of $-0.0047 \pm 0.0026 \text{ years}^{-1}$ and $-0.017 \pm 0.009 \text{ years}^{-1}$, respectively, and are ~ 2 – 3 times faster than those solely due to increasing atmospheric CO_2 . We attributed the rapid acidification to the increased dissolved inorganic carbon owing to a combination of ice melt-induced increased atmospheric CO_2 invasion and subsurface remineralization induced by a stronger surface biological production as a result of the increased inflow of the nutrient-rich Pacific water.

Plain Language Summary Anthropogenic CO_2 absorbed by the ocean leads to a lower pH and the calcium carbonate saturation state (Ω) and threatens the marine ecosystems state of healthiness via a process called ocean acidification (OA). The Arctic Ocean is particularly sensitive to OA because more CO_2 can be dissolved in cold water. This study used the observations collected over 17 years from 2002 to 2019 to estimate long-term trends of Ω_{arag} and pH in the Chukchi Sea. The results show that rapid acidification occurred throughout all water masses from 2002 to 2019, leading to or approaching aragonite undersaturation. The rapid acidification is attributed to the enhanced increasing concentration of dissolved inorganic carbon. While sea ice melt induced uptake of anthropogenic CO_2 partly explains the long-term acidification, the remainder is due to the increased nutrient-rich Pacific inflow water which promotes the high biological CO_2 utilization in the surface waters but leads to stronger subsurface acidification due to the regenerated CO_2 . We suggest that the acidity in Chukchi Arctic Shelf waters will increase in the future if the increased inflow of Pacific water continues.

1. Introduction

Since the industrial revolution, the decrease of pH and carbonate saturation state (Ω) caused by ocean uptake of anthropogenic CO_2 from the atmosphere, namely ocean acidification (OA), has become an important environmental issue that seriously threatens the marine ecosystem healthy and the development of human communities (Doney et al., 2009, 2020; Feely et al., 2004, 2009; Gattuso et al., 2015). It has been widely observed that the long-term OA rates are comparable to the rates predicted from the increase of atmospheric CO_2 across the global oceans (Bates, Astor, et al., 2014; Carter et al., 2017; Dore et al., 2009; Feely et al., 2012; Gregor & Gruber, 2021; Ishii et al., 2011; Murata et al., 2015; Murata & Saito, 2012; Oka et al., 2019; Ríos et al., 2015; Takahashi et al., 2014; Woosley et al., 2016). However, for the coastal oceans, observation-based assessment of OA and its driving mechanisms is limited due to the complexity of intertwined factors including anthropogenic forcing, natural variability, and local biogeochemical processes (Lui et al., 2015; Sarma et al., 2021; Wakita et al., 2021). Atmospheric circulation, mixing of water masses, and biogeochemical signals mitigate or amplify the atmospheric CO_2 increase-induced OA (Cai et al., 2011; Wakita et al., 2021), therefore it is difficult to decipher/validate OA with robust evidence.

© 2022. The Authors.

This is an open access article under the terms of the [Creative Commons Attribution License](#), which permits use, distribution and reproduction in any medium, provided the original work is properly cited.

Among the global oceans, the Arctic Ocean has a strong CO₂ absorption capacity due to its low temperature (Bates et al., 2006). Both observations and models have shown that the ice-free Arctic Ocean is the most susceptible region to OA and that it would be the first ocean basin to encounter severe undersaturation of aragonite calcium carbonate ($\Omega_{\text{arag}} < 1$) (Qi et al., 2017; Robbins et al., 2013; Terhaar et al., 2020; Yamamoto-Kawai et al., 2009). The decadal increase in sea-ice melt and riverine freshwater input contribute to the dilution of seawater and therefore lowers the concentrations of carbonate ion (CO₃²⁻), total alkalinity (TA), and calcium ion (Bates et al., 2009; Yamamoto-Kawai et al., 2009), resulting in a further decrease in pH and Ω_{arag} .

The Chukchi Sea, as an important inflow continental shelf of the Arctic Ocean, has experienced more dramatic climate-driven changes. Rapid sea-ice retreat (Screen & Simmonds, 2010; Wang & Overland, 2009) and increased inflow of nutrient-rich surface water from the Pacific Ocean (Woodgate & Rebecq, 2017; Woodgate et al., 2012) resulted in an increase in primary production (Lewis et al., 2020), and the increasing carbon sink accounting for more than 50% of the overall Arctic Ocean CO₂ sink and 8% of the global marginal sea CO₂ sink (Bates et al., 2006; Ouyang et al., 2020; Tu et al., 2021). Sea-ice loss also has substantial impacts on OA as it experiences extended ice-free periods during summers (as illustrated in Figure S1 in the Supporting Information S1). The emerging ice melt promotes primary production and CO₂ removal, which keeps high OA buffer capacity and oversaturated Ω_{arag} (>1) in the surface mixed layer. Meanwhile, ice melt is sometimes accompanied by the dissolution of CaCO₃ trapped in sea ice, which consumes CO₂ and alleviates acidification (Rysgaard et al., 2012). Although the concentration of dissolvable CaCO₃ is possibly low in sea ice (2–4 $\mu\text{mol L}^{-1}$) (Bates, Garley, et al., 2014; Rysgaard et al., 2012), the dissolution of CaCO₃ would increase TA and also the CO₂ buffering capacity, leading to enhanced atmospheric CO₂ uptake. On the contrary, sea-ice melt removes the barrier to air-sea gas exchange and promotes CO₂ uptake from the atmosphere, which potentially lowers surface pH and Ω_{arag} . In addition, increased microbial decay of organic matters in autumn and winter can strengthen the seasonal acidification by releasing CO₂ into the subsurface and bottom waters (Bates et al., 2009; Qi et al., 2020). In particular, close to 40% of the shelf bottom water was subject to Ω_{arag} of less than 1 and about 80% of the shelf bottom water was subject to Ω_{arag} of less than 1.5 in summertime during 2009–2011 summer (Bates et al., 2013). These ongoing changes imprinting on top of the accumulated anthropogenic CO₂ in the atmosphere make it more complicated to understand the mechanism and trend of OA in this climate-sensitive region.

On a decadal scale, the long-term OA trend in the Chukchi Sea can be attributed to a combination of several processes, including those increasing *acidity* (cooling-driven increased CO₂ solubility and atmospheric CO₂ uptake, and CO₂ released from respiration) and those decreasing *acidity* (warming-driven decreased CO₂ solubility and CO₂ outgassing, photosynthesis, and dilution by sea-ice melt water and river water) (Bates et al., 2009; Cai et al., 2010; Else et al., 2013; Jutterström & Anderson, 2010; Kaltin & Anderson, 2005; Rysgaard et al., 2007). However, the current status and long-term changes of OA in the Chukchi Sea are not well known due to limited observations collected from some sporadic cruises. Thus, it is of great importance to better understand how fast OA rates change in the Chukchi Sea and how the carbonate chemistry responds to climate-driven changes as the Chukchi Sea is one of the most productive ecosystems in the world with a high biodiversity and important commercial fisheries (Lewis et al., 2020).

In this study, we first examined the variations of pH_T and Ω_{arag} based on the data collected from multiple Arctic research cruises from 2002 to 2019 and then quantified the long-term trends of OA in the Chukchi Sea. Finally, we evaluated the links between the environmental changes and OA over the study period.

2. Data and Methods

2.1. Synthesis Data Set

Concentrations of total alkalinity (TA), dissolved inorganic carbon (DIC), dissolved oxygen (DO), nutrient, and auxiliary data (e.g., temperature and salinity) from water samples collected during multiple cruises, including SBI 2002, SBI 2004, CHINARE 2008, 2010, 2012, 2014, 2016, 2017, 2018 and 2019 (Figure 1, Figure S2 in the Supporting Information S1). The discrete samples from CHINARE cruises were collected by Niskin bottles on a CTD rosette package employing a SBE 911plus conductivity-temperature-depth (CTD) system. Samples were collected in borosilicate glass bottles and were preserved with HgCl₂. All samples were analyzed within 8 weeks after collection. DIC was measured from 0.75 mL water samples via acidification and subsequent quantification of released CO₂ by a non-dispersive infrared CO₂ analyzer (Apollo SciTech DIC analyzer, USA). TA was

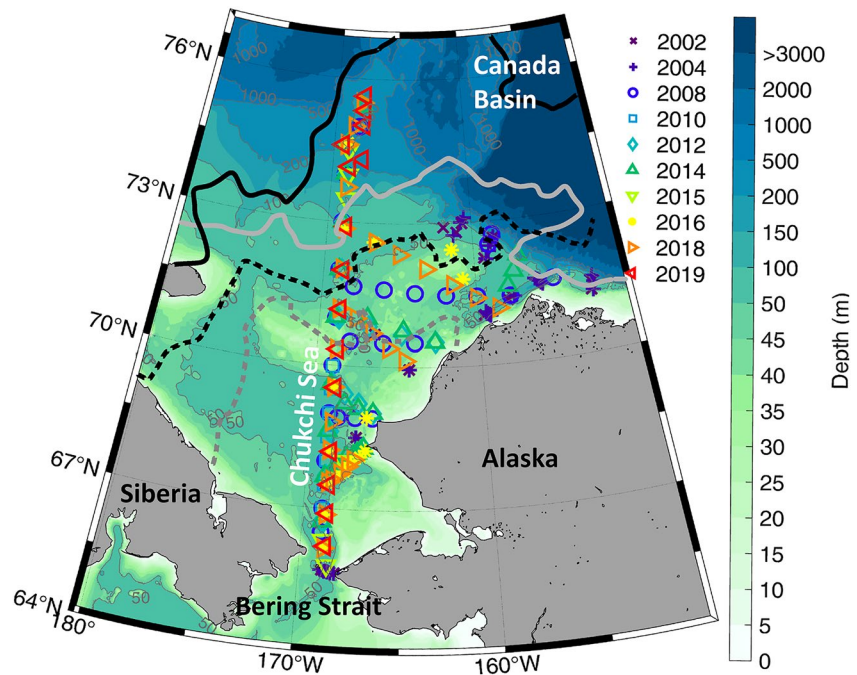


Figure 1. Map of the Chukchi Sea superimposed by topography. Different colors and symbols represent sampling stations in different years. The solid gray and black contours indicate the ice edge (15% ice concentration) in the first week of August 2002 and 2019, respectively; while the dashed contours indicate that in the first week of July. The daily sea ice concentration (SIC) data were obtained from the National Snow and Ice Data Center (NSIDC). The product is available at a horizontal resolution of 25 km on a polar stereographic projection (<https://nsidc.org/data/NSIDC-0079/versions/3>).

measured using the open-cell Gran titration method (Apollo SciTech Alkalinity analyzer, USA). Both DIC and TA were measured multiple times ($N \geq 3$) until the repeatability had a precision of better than 0.1% ($\pm 2 \mu\text{mol kg}^{-1}$). DIC and TA were calibrated using certified reference material (CRM) supplied by A.G. Dickson, Scripps Institution of Oceanography (USA). The DO concentration was determined using the automatic spectrophotometric Winkler titration system, with accuracy better than 1% (Pai et al., 1993).

2.2. Calculation of OA Parameters and AOU

pH and Ω_{arag} were calculated using version 1.1 of CO2SYS for Matlab (Heuven et al., 2011), with the carbonic acid dissociation constants K_1 and K_2 from Roy et al. (1993), K_{sp} from Mucci (1983), K_{SO_4} from Dickson (1990), and the total borate-salinity relationship from Lee et al. (2010). We used the dissociation constants (K_1 and K_2) of Roy et al. (1993) recommended by Chierici and Fransson (2009), which yields similar results to those using Mehrbach et al. (1973) as refit by Dickson and Millero (1987) described in Bates et al. (2009) and Chen et al. (2015) for low temperature waters. The pH was calculated in total scale (pH_T), for simplicity, the following ‘pH’ in this study refers to total scale pH at in situ temperature, unless otherwise specified. The associated uncertainty in CO2SYS calculations (due to uncertainties in TA, DIC, and dissociation constants) was estimated using the add-on from Orr et al. (2018).

The apparent oxygen utilization (AOU), used as a measurement of oxygen generation or consumption through biological processes, was calculated as the difference between the saturated oxygen concentration ($\text{O}_{2,\text{sat}}$) and the observed oxygen concentration ($\text{O}_{2,\text{obs}}$):

$$\text{AOU} = \text{O}_{2,\text{sat}} - \text{O}_{2,\text{obs}} \quad (1)$$

where $\text{O}_{2,\text{sat}}$ was calculated using the equations of H. E. Garcia and Gordon (1992); H. Garcia and Gordon (1993).

2.3. De-Seasonalization Procedure and Statistical Analyses

To avoid statistical bias due to seasonal variability to yearly means of observed variables, we applied de-seasonalization adjustments to both hydrographic and carbonate system parameters by assuming that the mean seasonality of climatology remained constant during the period of study. We used the method described in (Bates, Astor et al., 2014; Takahashi et al., 2009; Wakita et al., 2021). For example, the de-seasonalized monthly mean value of pH, pH_{des} , in each water masses was calculated as follows:

$$pH_{des} = pH_{obs} - pH_{mean}^{month} + pH_{mean}^{annual} \quad (2)$$

where pH_{obs} is the observed value of pH during a month, pH_{mean}^{month} is the monthly mean value of pH, and pH_{mean}^{annual} is the annual mean value. In this study, we used the summer mean value to substitute the annual mean due to the lack of data on yearly basis. This approach removes most of the seasonality observed and dampens potential seasonal bias of sampling ((Bates, Astor et al., 2014). In the following text we present the long-term trends of pH and Ω_{arag} with the de-seasonalized datasets.

We adopted the water mass classification used by Gong and Pickart (2015) and divided the Chukchi Sea waters into five main water masses, Pacific Winter Water (PWW), Alaska Coastal Water (ACW), Chukchi Summer Water (CSW), Early season Melt Water (ESMW), and Late-season Melt Water (LSMW) (Figure 2). The principles of doing water mass classification, uncertainty assessment, and sensitivity test are given in Text S1 in the Supporting Information S1.

2.4. Drivers of the Long-Term pH and Ω_{arag} Trends

We decomposed the variation of pH and Ω_{arag} into multiple components (T-temperature, S-salinity, TA-total alkalinity, DIC-dissolved inorganic carbon) to investigate the drivers of long-term changes by using a first-order Taylor-series deconvolution approach (Kwiatkowski & Orr, 2018):

$$dVar = \frac{\partial Var}{\partial T} \times dT + \frac{\partial Var}{\partial S} \times dS + \frac{\partial Var}{\partial DIC} \times dDIC + \frac{\partial Var}{\partial TA} \times dTA \quad (3)$$

where Var is the variable of pH or Ω_{arag} , and dVar is the change in variable. The partial derivatives were estimated based on the observed data assuming a 1‰ change (e.g., increase) on the relative parameters while keeping the other parameters constant (following Orr et al., 2015). Taking the estimation of $\frac{\partial pH}{\partial DIC}$ for example, the initial $pH_0 = f(T_0, S_0, DIC_0, TA_0)$ from CO2SYS calculation, the changed $pH_1 = f(T_0, S_0, DIC_1, TA_0)$, where $DIC_1 = 1.001 \times DIC_0$, thus, $\frac{\partial pH}{\partial DIC} = (pH_1 - pH_0) / (DIC_1 - DIC_0)$. For each derivative term, we used -0.0170 per °C, -0.0125 per psu (practical salinity units), 0.0026 per $\mu\text{mol kg}^{-1}$, and -0.0027 per $\mu\text{mol kg}^{-1}$, for $\frac{\partial pH}{\partial T}$, $\frac{\partial pH}{\partial S}$, $\frac{\partial pH}{\partial DIC}$, and $\frac{\partial pH}{\partial TA}$ respectively; and 0.0097 per °C, -0.0138 per psu, 0.0090 per $\mu\text{mol kg}^{-1}$, and -0.0085 per $\mu\text{mol kg}^{-1}$ for $\frac{\partial \Omega_{arag}}{\partial T}$, $\frac{\partial \Omega_{arag}}{\partial S}$, $\frac{\partial \Omega_{arag}}{\partial DIC}$, and $\frac{\partial \Omega_{arag}}{\partial TA}$, respectively.

We further accounted for the freshwater effect which changes S, TA, and DIC by adding a freshwater term (following Landschützer et al., 2018 and Ouyang et al., 2020):

$$dVar = \frac{\partial Var}{\partial T} \times dT + \frac{\partial Var}{\partial DIC} \times \frac{S}{S_0} \times dsDIC + \frac{\partial Var}{\partial TA} \times \frac{S}{S_0} \times dsTA + \frac{\partial Var}{\partial fw} \times dfw \quad (4)$$

$$\frac{\partial Var}{\partial fw} \times dfw = \left(\frac{\partial Var}{\partial DIC} \times \frac{sDIC}{S_0} + \frac{\partial Var}{\partial TA} \times \frac{sTA}{S_0} + \frac{\partial Var}{\partial S} \times \frac{S}{S_0} \right) \times dS \quad (5)$$

where S_0 is the mean salinity during the observation, sDIC and sTA are the salinity-normalized DIC and TA, respectively. We also estimated the temporal trends of pH and Ω_{arag} due to long-term changes in T, DIC, TA, and freshwater, input by taking a time derivative of and rearranging Equation 4 into:

$$\begin{aligned} \frac{dVar}{dt} = & \left(\beta_{SST} \times \frac{Var}{T} \times \frac{dT}{dt} \right) + \left(\beta_{DIC} \times \frac{Var}{DIC} \times \frac{dsDIC}{dt} \right) \\ & + \left(\beta_{TA} \times \frac{Var}{TA} \times \frac{dsTA}{dt} \right) + (\beta_{DIC} + \beta_{TA} + \beta_S) \times \frac{Var}{S_0} \times \frac{dS}{dt} \end{aligned} \quad (6)$$

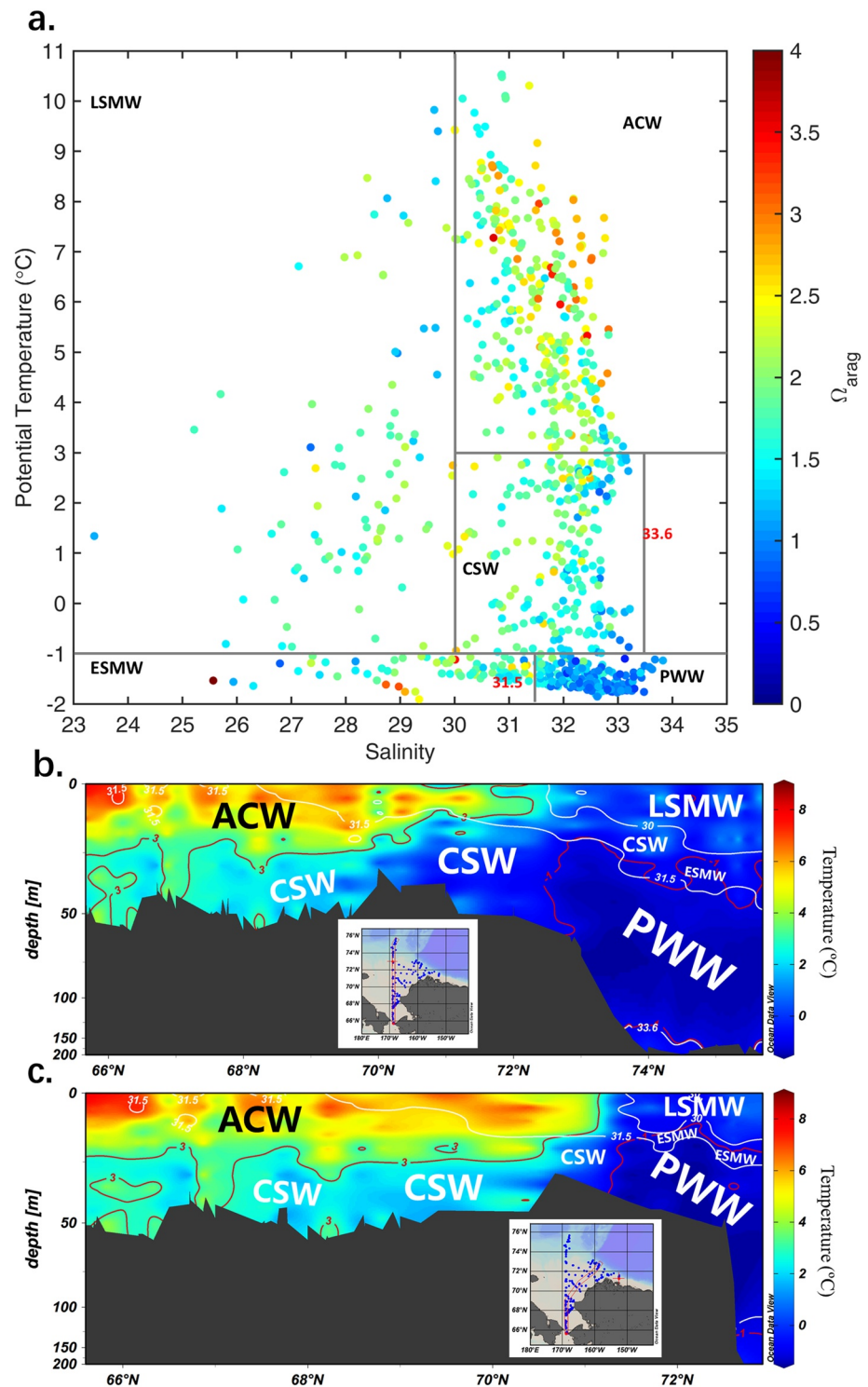


Figure 2. Classification and distribution of the water masses in the Chukchi Sea. (a) temperature-salinity diagram of the water masses. The color indicates aragonite saturation state. (b, c) vertical profiles of temperature (°C) (color contour and red contours) along the western (~169°W) and eastern cruise track from 2002 to 2019. Superimposed by salinity (white solid contours). The major water mass classes are labeled: Pacific Winter Water (PWW), Alaska Coastal Water (ACW), Chukchi Summer Water (CSW), Early season Melted Water (ESMW), and Late-season Melted Water (LSMW).

where β is the sensitivity of pH to T, DIC, and TA (in the case of Ω_{arag} , the sensitivity is written as γ) (Egleston et al., 2010). For instance, the sensitivity of pH to DIC is $\beta_{\text{DIC}} = \left(\frac{\partial \text{pH}}{\partial \text{DIC}}\right) / \left(\frac{\partial \text{pH}}{\partial \text{DIC}}\right)$. T, DIC, TA, S_0 , and Var are the long-term means.

The salinity-normalized DIC and TA were calculated accounting for the riverine and ice meltwater impacts (Friis et al., 2003), using the following equations:

$$s\text{DIC} = \frac{\text{DIC} - \text{DIC}_{S=0}}{S} \times S_0 + \text{DIC}_{S=0} \quad (7)$$

$$s\text{TA} = \frac{\text{TA} - \text{TA}_{S=0}}{S} \times S_0 + \text{TA}_{S=0} \quad (8)$$

The values of $\text{DIC}_{S=0}$ and $\text{TA}_{S=0}$ were identified for each water mass. We fit the linear regression between TA and salinity, and took the y-intercept value (TA value at $S = 0$) as the $\text{TA}_{S=0}$. The $\text{TA}_{S=0}$ for PWW, ACW, CSW, ESMW, and LSMW are 814.2, 1136.7, 995.9, 794.8, and 103.7 $\mu\text{mol kg}^{-1}$, respectively. The former four relatively higher $\text{TA}_{S=0}$ values are due to the riverine input, while the lowest $\text{TA}_{S=0}$ in LSMW is due to ice meltwater (Cai et al., 2010). We therefore converted each $\text{TA}_{S=0}$ to $\text{DIC}_{S=0}$ with the characteristic ratios ($\text{TA}/\text{DIC} = 0.956$ for river waters and $\text{TA}/\text{DIC} = 104/59.8 = 1.739$ for ice meltwater; see in the Supporting Information S1 in Cai et al., 2010).

We further separate the drivers of the observed pH and Ω_{arag} changes into thermal and non-thermal components. The thermal component is driven by changes in seawater temperature (the first term on the right-hand side of Equation 4), and the non-thermal component is driven by changes in sDIC, sTA, and salinity (inferred by freshwater input due to sea-ice melt and river input, which not only dilutes the surface salinity but also affects the carbonate chemistry).

In addition, we also quantified the effects of specific biogeochemical processes (e.g., air-sea CO_2 exchange, photosynthesis/respiration) on altering pH and Ω_{arag} . Since air-sea CO_2 gas exchange does not change TA, photosynthesis/respiration only slightly changes TA, both these two processes affect pH and Ω_{arag} via changes in DIC. The contribution of photosynthesis/respiration to DIC and thus pH and Ω_{arag} is calculated from proxies of $[\text{NO}_3 + \text{NO}_2]$ concentration and AOU. The biological effect on DIC could be inferred based on the classical Redfield ratio of $\text{O}/\text{C}/\text{N} = -138/106/16$.

The contribution of air-sea CO_2 exchange to DIC increase can be estimated from CO_2 flux:

$$d\text{DIC}_{\text{ex}} = \text{FCO}_2 / \text{MLD} \quad (9)$$

where $d\text{DIC}_{\text{ex}}$ is the change in DIC attributed to air-sea CO_2 exchange, FCO_2 is the air-sea CO_2 flux, and MLD is the mixed layer depth (data adopted from Tu et al., 2021). The following equation shows the calculations of FCO_2 :

$$\text{FCO}_2 = f \times k \times K_H \times \Delta p\text{CO}_2 \quad (10)$$

where f is the correction term for sea ice, $f = (1 - \text{ice}\%)$; k and K_H are CO_2 gas transfer velocity and the solubility of CO_2 (calculated from temperature and salinity following Weiss, 1974), respectively. The value of k is calculated with the monthly second moment of wind speed at 10 m in height, $\langle U_{10}^2 \rangle$, as suggested by Wanninkhof (2014):

$$k = -0.251 \times \langle U_{10}^2 \rangle \times (\text{Sc}/660)^{-1/2} \quad (11)$$

where Schmidt number (Sc) is temperature-dependent for CO_2 in seawater, computed from SST.

3. Results and Discussion

3.1. Distribution of pH and Ω_{arag} in Different Water Masses

The highest Ω_{arag} (2.11 ± 0.11) is found in the ACW, which is also accompanied by medium pH (8.16 ± 0.11) (Table S1 in the Supporting Information S1). The ACW is the warmest water in the eastern Chukchi Sea originating from the Alaska coastal region south of Bering Strait. Approximately one-third of the Chukchi Sea is filled with ACW (Figures 2b and 2c; Refs). ACW often enters the Chukchi Sea in mid-to-late summer and is

characterized by $\theta \geq 3^{\circ}\text{C}$ and $S \geq 30$ (Figure 2a). The maximum temperature of ACW can reach up to $7\text{--}10^{\circ}\text{C}$ in August–September (Figure 2a). Low AOU value (averaged $17 \mu\text{mol kg}^{-1}$) means that primary production has offset oxygen utilization in ACW, which results in highest Ω_{arag} among the five water masses (Table S1 in the Supporting Information S1).

The lowest Ω_{arag} (1.09 ± 0.29) and pH (7.97 ± 0.11) values are found in the Pacific Winter Water (PWW) (Table S1 in the Supporting Information S1). PWW occupies one-quarter to one-third of the water column in the Chukchi Sea (Figures 2b and 2c) and is characterized by low temperatures ($-1.57 \pm 0.18^{\circ}\text{C}$), high nutrient concentrations, and high CO_2 due to remineralization of organic matter (Qi et al., 2017; Wynn et al., 2016; Yamamoto-Kawai et al., 2009).

The other three water masses, ESMW, LSMW, and CSW are greatly affected by seasonal sea-ice variation and primary production (Robbins et al., 2013; Yamamoto-Kawai et al., 2009). Dilution by sea ice and biological production impact pH and Ω_{arag} , and its large variability is marked by dramatic fluctuations in standard deviations (Table S1 in the Supporting Information S1).

3.2. Decadal Change of pH and Ω_{arag} in Different Water Masses

We now investigate the temporal variation (long-term trend) of pH and Ω_{arag} data based on the de-seasonalized monthly mean values of each variable. Our results reveal a rapid acidification in the Chukchi Sea with a mean annual change rate of -0.0047 ± 0.0026 for pH and -0.017 ± 0.009 for Ω_{arag} from 2002 to 2019 (averaged values of all water masses in Figure 3). The mean annual OA rates are highest in the ESMW and LSMW (-0.0060 to -0.0086 for pH and -0.0247 to -0.0282 for Ω_{arag}), and lowest in the PWW (-0.0033 ± 0.0031 for pH and -0.0085 ± 0.0071 for Ω_{arag}) with significant aragonite undersaturation ($\Omega_{\text{arag}} < 1$) were observed after 2010 (Figure 3).

Note that when the original monthly means were used to estimate the decreasing rates of pH and Ω_{arag} , they resulted in rates around twice faster than those based on the de-seasonalized means (Figure 3 vs. Figure S3 in the Supporting Information S1). We attribute this difference to increased observations in late summer months (late August and September) since 2010 (Figure S4 in the Supporting Information S1), during which the seasonal acidification is more severe due to stronger respiration in the subsurface waters. To avoid statistical bias due to seasonal variability to yearly means of observed variables, it is necessary to perform the de-seasonalization for the long-term trends in pH and Ω_{arag} . Not adjusting for seasonality would risk overestimating the acidification rates (Figure S3 in the Supporting Information S1). The results also show that the removal of some portion of the data or cruise also has a negligible impact on the derived pH and Ω_{arag} trends, indicating the good representativeness and robustness of the synthesis results (Figures S5 and S6 in the Supporting Information S1).

3.3. Processes Controlling the Long-Term Trends in pH and Ω_{arag}

We now quantitatively evaluate how pH and Ω_{arag} respond to environmental change. The decomposition shows that thermal effect (warming rate of $0.008^{\circ}\text{C yr}^{-1}$ over 2002–2019, Figure S7 in the Supporting Information S1) only induces slight changes in the rate of pH and Ω_{arag} across the five water masses in the Chukchi Sea, which are negligible compared to their overall changes and the total non-thermal effect (Figure 4).

Among the non-thermal factors, sDIC is the dominant driver for the long-term decrease in pH and Ω_{arag} across the five water masses, while salinity effect is always negligible (Figure 4). The contribution of sTA differs among water masses, that is, negligible in ACW, CSW, and PWW, but significantly increases pH and Ω_{arag} in ESMW and LSMW.

For the water masses of PWW, CSW, and ACW, the net average increase in sDIC (Figure S8 in the Supporting Information S1) lead to an average decrease in pH and Ω_{arag} by $-0.0033 \text{ years}^{-1}$ and $-0.0104 \text{ years}^{-1}$, respectively. The contribution of freshwater input (salinity) and sTA are small (Figure 4). As a result, the cumulative changes from thermal and non-thermal components in pH and Ω_{arag} are $-0.0035 \text{ years}^{-1}$ and $-0.0106 \text{ years}^{-1}$, respectively, which are consistent with the observed long-term OA trends (accounting for $103\% \pm 11\%$ for pH and $121\% \pm 36\%$ for Ω_{arag}) (Figure 4). In the ACW, the CO_2 sink has increased over the past two decades (Tu et al., 2021; Zheng et al., 2021). The increased vertical flux and respiration of organic matter below the pycnocline introduces more additional CO_2 into the subsurface CSW and PWW waters (aerobic respiration; Stabeno

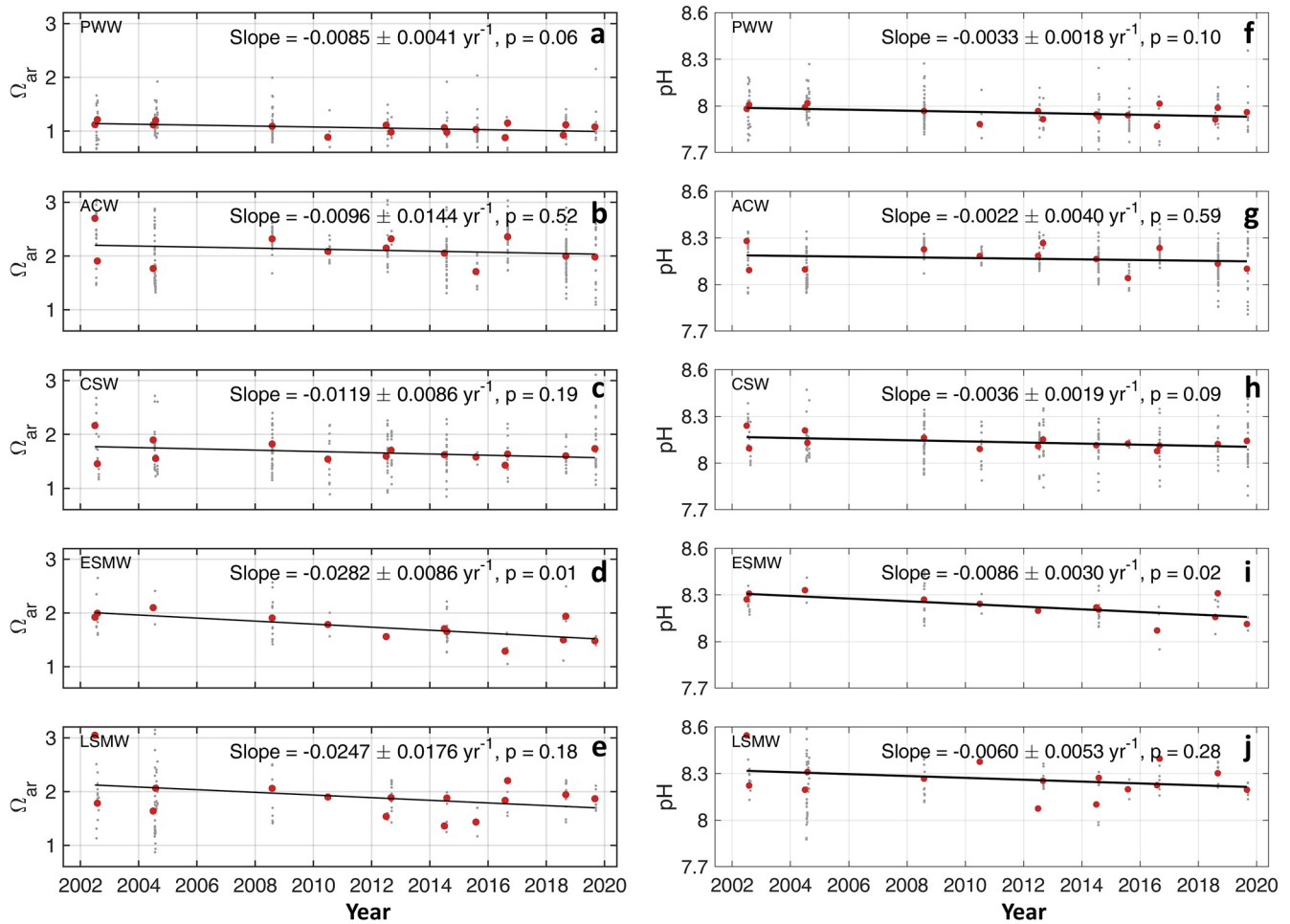


Figure 3. Estimated rates of yearly change in seawater Ω_{arag} and pH throughout the water column in the Chukchi Sea. The water masses include Pacific Winter Water (PWW), Alaska Coastal Water (ACW), Chukchi Summer Water (CSW), Early season Melt Water (ESMW), and Late-season Melt Water (LSMW).

et al., 2018), thereby decreasing pH and Ω_{arag} and enhancing subsurface and near-bottom acidification over the past 17 years.

Upon moving northwards to the shelf break and slope, where large portion (>90%) of the upper layer is comprised of ESMW and LSMW (Figures 2b and 2c), the sea-ice edge has retreated northwards rapidly from 2002 to 2019 (Figure 1 and Figure S1 in the Supporting Information S1). The net increase in sDIC (Figure S8 in the Supporting Information S1) could lead to large decreases in pH and Ω_{arag} of $-0.0148 \text{ years}^{-1}$ and $-0.0465 \text{ years}^{-1}$ (Figure 4), while increase in sTA could also offset those changes by around half (increasing pH and Ω_{arag} by $0.0086 \text{ years}^{-1}$ and $0.0025 \text{ years}^{-1}$, respectively) (Figure 4; see Equation 6 for detailed calculations). The contribution of freshwater input (salinity) only changes pH by $0.00018 \text{ years}^{-1}$ and Ω_{arag} by $-0.0018 \text{ years}^{-1}$. As a result, the cumulative changes from thermal and non-thermal components in pH and Ω_{arag} are $-0.0085 \text{ years}^{-1}$ and $-0.0265 \text{ years}^{-1}$, respectively, which is also consistent with the observed long-term OA trends (account for 116% for pH and 97% for Ω_{arag}) (Figure 4). We explored the possible explanations for the sizable effect from TA changes, and found that dissolution of CaCO_3 during sea-ice melt is the most likely cause, subjected to the limited data, further studies such as collect the data of Ca^{2+} are needed to fully unveil the CaCO_3 cycle during ice melt-formation processes.

We further investigate the primary mechanisms driving the long-term DIC increase. Strengthened air-sea CO_2 exchange due to sea-ice melt and enhanced organic matter respiration due to inflow of Pacific waters are the most likely causes. The increased uptake of atmospheric CO_2 from 2002 to 2019 would reduce pH and Ω_{arag} by $-0.0038 \text{ years}^{-1}$ and $-0.012 \text{ years}^{-1}$ (following Tu et al., 2021), respectively, which contributes to about 79% and 71% of the total pH and Ω_{arag} long-term trends in the Chukchi Sea. The contribution from respiration was

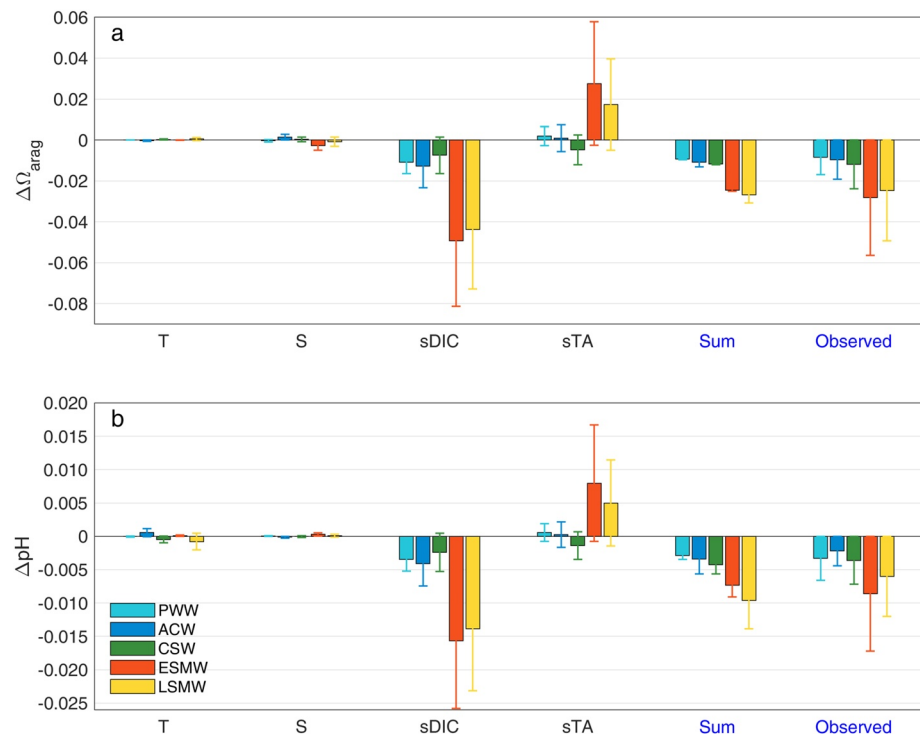


Figure 4. The quantification of each driver on altering the Ω_{arag} and pH yearly rates. Colors indicate different water masses. The 'sum' term is the accumulative effect from T, S, sDIC, and sTA, and the 'observed' term is the observed yearly rate.

then estimated from indicators of NO_x^- ($\text{NO}_3^- + \text{NO}_2^-$) and apparent oxygen utilization (AOU), which increased by 0.14 and $0.76 \mu\text{mol kg}^{-1} \text{yr}^{-1}$ from 2002 to 2019 (Figure S9 in the Supporting Information S1). Based on the Redfield ratio of $\text{O/C/N} = -138/106/16$ and DIC changes, the corresponding pH changes are -0.0016 (AOU-derived) to -0.025 (NO_x -derived) and the corresponding Ω_{arag} changes are -0.013 (AOU-derived) to -0.0078 (NO_x -derived). These respectively contribute to 35%–52% and 47%–76% of the total pH and Ω_{arag} long-term trends in the Chukchi Sea.

4. Summary and Concluding Remarks

Based on the 17-year data set, we found a distinct acidification with a mean annual change rate of -0.0047 ± 0.0026 for pH and -0.017 ± 0.009 for Ω_{arag} from 2002 to 2019 throughout the whole water columns in the Chukchi Sea. These OA rates are approximately 2–3 times faster than the OA rate driven only by increased atmospheric CO_2 in the open oceans (Bates, Astrol, et al., 2014; Wakita et al., 2021). The rapid acidification was induced by the rapid increase of DIC, with compounding effects from increased atmospheric CO_2 uptake and stronger organic matter remineralization. This is in stark contrast to that in the global open ocean, where the atmospheric forcing is similar to coastal oceans but the intensity of biological CO_2 uptake is substantially lower.

This study also shows that the undersaturation with respect to aragonite in PWW has continued for ~ 10 years, beginning in 2010. If this trend continues and the sea surface $p\text{CO}_2$ values follow the atmospheric $p\text{CO}_2$, we suggest that the other water masses are expected to encounter undersaturation ($\Omega_{\text{arag}} < 1$) as early as 2036. In the future, increased atmospheric CO_2 and prolonged summertime ice free period will continue to decrease pH and Ω_{arag} . In the meantime, the nutrient-rich Pacific inflow will also stimulate the biological activity and surface CO_2 uptake in the Chukchi Sea, but release more CO_2 into the subsurface water from remineralization. Although at present there is no prediction for future changes of the Arctic Ocean circulation pattern regarding the Pacific inflow water, it is suggested that all the processes above will contribute to severe acidification in the Chukchi Sea, which eventually threatens the shelled organisms and other parts of the ecosystem.

Data Availability Statement

The data synthesis used in this manuscript can be accessed at the Mendeley data repository, which can be found at <https://data.mendeley.com/datasets/vytzhmm254/1> (doi:<https://doi.org/10.17632/vytzhmm254.1>).

Acknowledgments

We express our sincere gratitude to the crews of the Chinese National Arctic Research Expedition on board R/V Xuelong for their supports, the researchers during the cruises for their sampling and measurements, as well as National Arctic and Antarctic Data Center from China. This work was funded by the National Key Research and Development Program of China (2019YFE0114800), the National Natural Science Foundation of China (41630969, 41941013, 42176230), Key Deployment Project of Centre for Ocean Mega-Research of Science, CAS (Grant No. COMS2020Q12), and the Scientific Research Foundation of Third Institute of Oceanography, MNR (Grant No. 2019032). W.-J.C. and Z.O. are supported by NSF (OPP-1926158). This is PMEL contribution number 5307 from the NOAA Pacific Marine Environmental Laboratory.

References

- Bates, N. R., Astor, Y. M., Church, M. J., Currie, K., Dore, J. E., Gonzalez-Davila, M., et al. (2014). A time-series view of changing ocean chemistry due to ocean uptake of anthropogenic CO₂ and ocean acidification. *Oceanography*, 27(1), 126–141. <https://doi.org/10.5670/oceanog.2014.16>
- Bates, N. R., Garley, R., Frey, K. E., Shake, K. L., & Mathis, J. T. (2014). Sea-ice melt CO₂–carbonate chemistry in the western Arctic Ocean: Meltwater contributions to air–sea CO₂ gas exchange, mixed-layer properties and rates of net community production under sea ice. *Biogeosciences*, 11(23), 6769–6789. <https://doi.org/10.5194/bg-11-6769-2014>
- Bates, N. R., Mathis, J. T., & Cooper, L. W. (2009). Ocean acidification and biologically induced seasonality of carbonate mineral saturation states in the western Arctic Ocean. *Journal of Geophysical Research Oceans*, 114(C11). <https://doi.org/10.1029/2008jc004862>
- Bates, N. R., Moran, S. B., Hansell, D. A., & Mathis, J. T. (2006). An increasing CO₂ sink in the Arctic Ocean due to sea-ice loss. *Geophysical Research Letters*, 33(23). <https://doi.org/10.1029/2006gl027028>
- Bates, N. R., Orchowka, M. I., Garley, R., & Mathis, J. T. (2013). Summertime calcium carbonate undersaturation in shelf waters of the western Arctic Ocean—how biological processes exacerbate the impact of ocean acidification. *Biogeosciences*, 10(8), 5281–5309. <https://doi.org/10.5194/bg-10-5281-2013>
- Cai, W. J., Chen, L., Chen, B., Gao, Z., Lee, S. H., Chen, J., et al. (2010). Decrease in the CO₂ uptake capacity in an ice-free Arctic Ocean basin. *Science*, 329(5991), 556–559. <https://doi.org/10.1126/science.1189338>
- Cai, W. J., Hu, X., Huang, W.-J., Murrell, M. C., Lehrter, J. C., Lohrenz, S. E., et al. (2011). Acidification of subsurface coastal waters enhanced by eutrophication. *Nature Geoscience*, 4(11), 766–770. <https://doi.org/10.1038/ngeo1297>
- Carter, B. R., Feely, R. A., Mecking, S., Cross, J. N., Macdonald, A. M., Siedlecki, S. A., et al. (2017). Two decades of Pacific anthropogenic carbon storage and ocean acidification along GO-SHIP sections P16 and P02. *Global Biogeochemical Cycles*, 31(2). <https://doi.org/10.1002/2016GB005485>
- Chen, B., Cai, W. J., & Chen, L. (2015). The marine carbonate system of the Arctic Ocean: Assessment of internal consistency and sampling considerations, summer 2010. *Marine Chemistry*, 176, 174–188. <https://doi.org/10.1016/j.marchem.2015.09.007>
- Chierici, M., & Fransson, A. (2009). Calcium carbonate saturation in the surface water of the Arctic Ocean: Undersaturation in freshwater influenced shelves. *Biogeosciences*, 6(11), 2421–2431. <https://doi.org/10.5194/bg-6-2421-2009>
- Dickson, A. G. (1990). Standard potential of the reaction: AgCl (s) + 1/2H₂ (g) = Ag (s) + HCl (aq), and the standard acidity constant of the ion HSO₄⁻ in synthetic Sea water from 273.15 to 318.15 K. *Journal of Chemical Thermodynamics*, 22(2), 113–127. [https://doi.org/10.1016/0021-9614\(90\)90074-Z](https://doi.org/10.1016/0021-9614(90)90074-Z)
- Dickson, A. G., & Millero, F. J. (1987). A comparison of the equilibrium constants for the dissociation of carbonic acid in seawater media. *Deep-Sea Research Part A. Oceanographic Research Papers*, 34(10), 1733–1743. [https://doi.org/10.1016/0198-0149\(87\)90021-5](https://doi.org/10.1016/0198-0149(87)90021-5)
- Doney, S. C., Busch, D. S., Cooley, S. R., & Kroeker, K. J. (2020). The impacts of Ocean acidification on marine ecosystems and Reliant human communities. *Annual Review of Environment and Resources*, 45, 11–111.30. <https://doi.org/10.1146/annurev-environ-012320-083019>
- Doney, S. C., Fabry, V. J., Feely, R. A., & Kleypas, J. A. (2009). Ocean acidification: The other CO₂ problem. *Annual Review of Marine Science*, 1, 169–192. <https://doi.org/10.1146/annurev.marine.010908.163834>
- Dore, J. E., Roger, L., Sadler, D. W., Church, M. J., & Karl, D. M. (2009). Physical and biogeochemical modulation of ocean acidification in the central North Pacific. *Proc Natl Acad Sci U S A*, 106(30), 12235–12240. <https://doi.org/10.1073/pnas.0906044106>
- Egleston, E. S., Sabine, C. L., & Morel, F. M. M. (2010). Revelle revisited: Buffer factors that quantify the response of Ocean chemistry to changes in DIC and alkalinity. *Global Biogeochemical Cycles*, 24(1). <https://doi.org/10.1029/2008GB003407>
- Else, B. G. T., Galley, R. J., Lansard, B., Barber, D. G., Brown, K., Miller, L. A., et al. (2013). Further observations of a decreasing atmospheric CO₂ uptake capacity in the Canada Basin (Arctic Ocean) due to sea ice loss. *Geophysical Research Letters*, 40(6), 1132–1137. <https://doi.org/10.1002/grl.50268>
- Feely, R. A., Doney, S. C., & Cooley, S. R. (2009). Ocean acidification: Present conditions and future changes in a high-CO₂ world. *Oceanography*, 22(4), 36–47. <https://doi.org/10.5670/oceanog.2009.95>
- Feely, R. A., Sabine, C. L., Byrne, R. H., Millero, F. J., Dickson, A. G., Wanninkhof, R., et al. (2012). Decadal changes in the aragonite and calcite saturation state of the Pacific Ocean. *Global Biogeochemical Cycles*, 26(3). <https://doi.org/10.1029/2011gb004157>
- Feely, R. A., Sabine, C. L., Lee, K., Berelson, W., Kleypas, J., Fabry, V. J., & Millero, F. J. (2004). Impact of anthropogenic CO₂ on the CaCO₃ system in the oceans. *Science*, 305(5682), 362–366. <https://doi.org/10.1126/science.1097329>
- Friis, K., Körtzinger, A., & Wallace, D. W. (2003). The salinity normalization of marine inorganic carbon chemistry data. *Geophysical Research Letters*, 30(2), 1080. <https://doi.org/10.1029/2002GL015898>
- Garcia, H., & Gordon, L. (1993). Erratum: Oxygen solubility in seawater: Better fitting equations. *Limnology & Oceanography*, 38(3), 656.
- Garcia, H. E., & Gordon, L. I. (1992). Oxygen solubility in seawater: Better fitting equations. *Limnology & Oceanography*, 37(6), 1307–1312. <https://doi.org/10.4319/lo.1992.37.6.1307>
- Gattuso, J.-P., Magnan, A., Bille, R., Cheung, W. W. L., Howes, E. L., Joos, F., et al. (2015). Contrasting futures for ocean and society from different anthropogenic CO₂ emission scenarios. *Science*, 349(6243), aac4722. <https://doi.org/10.1126/science.aac4722>
- Gong, D., & Pickart, R. S. (2015). Summertime circulation in the eastern Chukchi Sea. *Deep-Sea Research Part II*, 118(AUG), 18–31. (PT.A). <https://doi.org/10.1016/j.dsr2.2015.02.006>
- Gregor, L., & Gruber, N. (2021). OceanSODA-ETHZ: A global gridded data set of the surface ocean carbonate system for seasonal to decadal studies of Ocean acidification. *Earth System Science Data*, 13(2), 777–808. <https://doi.org/10.5194/essd-13-777-2021>
- Heuven, S. V., Pierrot, D., Rae, J., Lewis, E., & Wallace, D. (2011). CO₂SYS v 1.1, MATLAB program developed for CO₂ system calculations. https://doi.org/10.3334/CDIAC/otg.CO2SYS_MATLAB_v1.1
- Ishii, M., Kosugi, N., Sasano, D., Shu, S., Midorikawa, T., & Inoue, H. Y. (2011). ocean acidification off the south coast of Japan: A result from time series observations of CO₂ parameters from 1994 to 2008. *Journal of Geophysical Research Oceans*, 116(C6). <https://doi.org/10.1029/2010JC006831>

- Jutterström, S., & Anderson, L. G. (2010). Uptake of CO₂ by the Arctic Ocean in a changing climate. *Marine Chemistry*, 122(1–4), 96–104. <https://doi.org/10.1016/j.marchem.2010.07.002>
- Kaltin, S., & Anderson, L. G. (2005). Uptake of Atmospheric carbon dioxide in Arctic shelf seas: Evaluation of the relative importance of processes that influence pCO₂ in water transported over the Bering-Chukchi Sea shelf. *Marine Chemistry*, 94, 67–79. <https://doi.org/10.1016/j.marchem.2004.07.010>
- Kwiatkowski, L., & Orr, J. C. (2018). Diverging seasonal extremes for ocean acidification during the twenty-first century. *Nature Climate Change*, 8(2), 141–145. <https://doi.org/10.1038/s41558-017-0054-0>
- Landschützer, P., Gruber, N., Bakker, D. C. E., Stemmler, I., & Six, K. D. (2018). Strengthening seasonal marine CO₂ variations due to increasing atmospheric CO₂. *Nature Climate Change*, 8, 146–150. <https://doi.org/10.1038/s41558-017-0057-x>
- Lee, K., Kim, T. W., Byrne, R. H., Millero, F. J., Feely, R. A., & Liu, Y. M. (2010). The universal ratio of boron to chlorinity for the North Pacific and North Atlantic oceans. *Geochimica et Cosmochimica Acta*, 74(6), 1801–1811. <https://doi.org/10.1016/j.gca.2009.12.027>
- Lewis, K. M., van Dijken, G. L., & Arrigo, K. R. (2020). Changes in phytoplankton concentration now drive increased Arctic Ocean primary production. *Science*, 369(6500), 198–202. <https://doi.org/10.1126/science.aay8380>
- Lui, H. K., Chen, C. T. A., Lee, J., Wang, S. L., Gong, G. C., Bai, Y., & He, X. (2015). Acidifying intermediate water accelerates the acidification of seawater on shelves: An example of the East China Sea. *Continental Shelf Research*, 111, 223–233. <https://doi.org/10.1016/j.csr.2015.08.014>
- Mehrbach, C., Culbertson, C. H., Hawley, J. E., & Pytkowicz, R. M. (1973). Measurement of the apparent dissociation constants of carbonic acid in seawater at atmospheric pressure. *Limnology & Oceanography*, 18(6), 897–907. <https://doi.org/10.4319/lo.1973.18.6.0897>
- Mucci, A. (1983). The solubility of calcite and aragonite in seawater at various salinities, temperatures and one atmosphere total pressure. *Amer. J.*, 283(7), 14–799. <https://doi.org/10.2475/ajs.283.7.780>
- Murata, A., Hayashi, K., Kumamoto, Y., & Sasaki, K.-i. (2015). Detecting the progression of ocean acidification from the saturation state of CaCO₃ in the subtropical South Pacific. *Global Biogeochemical Cycles*, 29(4), 463–475. <https://doi.org/10.1002/2014gb004908>
- Murata, A., & Saito, S. (2012). Decadal changes in the CaCO₃ saturation state along 179°E in the Pacific Ocean. *Geophysical Research Letters*, 39(12). <https://doi.org/10.1029/2012gl052297>
- Oka, E., Yamada, K., Sasano, D., Enyo, K., Nakano, T., & Ishii, M. (2019). Remotely forced decadal physical and biogeochemical variability of north Pacific subtropical mode water over the last 40 years. *Geophysical Research Letters*, 46(3), 1555–1561. <https://doi.org/10.1029/2018GL081330>
- Orr, J. C., Epitalon, J. M., Dickson, A. G., & Gattuso, J. P. (2018). Routine uncertainty propagation for the marine carbon dioxide system. *Marine Chemistry*, 207, 84–107. <https://doi.org/10.1016/j.marchem.2018.10.006>
- Orr, J. C., Epitalon, J. M., & Gattuso, J. P. (2015). Comparison of ten packages that compute ocean carbonate chemistry. *Biogeosciences*, 12(4), 1483–1510. <https://doi.org/10.5194/bg-12-1483-2015>
- Ouyang, Z., Qi, D., Chen, L., Takahashi, T., Zhong, W., DeGrandpre, M. D., et al. (2020). Sea-ice loss amplifies summertime decadal CO₂ increase in the western Arctic Ocean. *Nature Climate Change*, 10(7), 678–684. <https://doi.org/10.1038/s41558-020-0784-2>
- Pai, S.-C., Gong, G.-C., & Liu, K.-K. (1993). Determination of dissolved oxygen in seawater by direct spectrophotometry of total iodine. *Marine Chemistry*, 41(4), 343–351. [https://doi.org/10.1016/0304-4203\(93\)90266-Q](https://doi.org/10.1016/0304-4203(93)90266-Q)
- Qi, D., Chen, B., Chen, L., Lin, H., Gao, Z., Sun, H., et al. (2020). Coastal acidification induced by biogeochemical processes driven by sea-ice melt in the western Arctic Ocean. *Polar Science*, 23, 100504. <https://doi.org/10.1016/j.polar.2020.100504>
- Qi, D., Chen, L., Chen, B., Gao, Z., Zhong, W., Feely, R. A., et al. (2017). Increase in acidifying water in the western Arctic Ocean. *Nature Climate Change*, 7(3), 195–199. <https://doi.org/10.1038/nclimate3228>
- Ríos, A. F., Resplandy, L., García-Ibáñez, M. I., Fajar, N. M., Velo, A., Padin, X. A., et al. (2015). Decadal acidification in the water masses of the Atlantic Ocean. *Proceedings of the National Academy of Sciences*, 112(32), 9950–9955. <https://doi.org/10.1073/pnas.1504613112>
- Robbins, L. L., Wynn, J. G., Lisle, J. T., Yates, K. K., Knorr, P. O., Byrne, R. H., et al. (2013). Baseline monitoring of the Western Arctic Ocean estimates 20% of Canadian Basin surface waters are undersaturated with respect to aragonite. *PloS one*, 8(9), e73796. <https://doi.org/10.1371/journal.pone.0073796>
- Roy, R., Roy, L., Vogel, K., Moore, C., Pearson, T., Good, C., et al. (1993). Determination of the ionization constants of carbonic acid in seawater. *Marine Chemistry*, 44, 249–267. [https://doi.org/10.1016/0304-4203\(93\)90207-5](https://doi.org/10.1016/0304-4203(93)90207-5)
- Rysgaard, S., Glud, R. N., Lennert, K., Cooper, M., Halden, N., Leakey, R. J. G., et al. (2012). Ikaite crystals in melting sea ice – Implications for pCO₂ and pH levels in Arctic surface waters. *The Cryosphere*, 6(4), 901–908. <https://doi.org/10.5194/tc-6-901-2012>
- Rysgaard, S., Glud, R. N., Sejr, M. K., Bendtsen, J., & Christensen, P. B. (2007). Inorganic carbon transport during sea ice growth and decay: A carbon pump in polar seas. *Journal of Geophysical Research*, 112, C03016. <https://doi.org/10.1029/2006jc003572>
- Sarma, V. V. S. S., Krishna, M. S., Srinivas, T. N. R., Kumari, V. R., Yadav, K., & Kumar, M. D. (2021). Elevated acidification rates due to deposition of atmospheric pollutants in the coastal Bay of Bengal. *Geophysical Research Letters*, 48(16). <https://doi.org/10.1029/2021GL095159>
- Screen, J. A., & Simmonds, I. (2010). The central role of diminishing sea ice in recent Arctic temperature amplification. *Nature*, 464(7293), 1334–1337. <https://doi.org/10.1038/nature09051>
- Stabeno, P., Kachel, N., La Dd, C., & Woodgate, R. (2018). Flow patterns in the eastern Chukchi Sea: 2010–2015. *Journal of Geophysical Research*, 123, 1177–1195. <https://doi.org/10.1002/2017JC013135>
- Takahashi, T., Sutherland, S. C., Chipman, D. W., Goddard, J. G., Ho, C., Newberger, T., et al. (2014). Climatological distributions of pH, pCO₂, total CO₂, alkalinity, and CaCO₃ saturation in the global surface ocean, and temporal changes at selected locations. *Marine Chemistry*, 164, 95–125. <https://doi.org/10.1016/j.marchem.2014.06.004>
- Takahashi, T., Sutherland, S. C., Wanninkhof, R., Sweeney, C., Feely, R. A., Chipman, D. W., et al. (2009). Climatological mean and decadal change in surface ocean pCO₂ and net sea–air CO₂ flux over the global oceans. *Deep-Sea Research Part II*, 56(8), 554–577. <https://doi.org/10.1016/j.dsr2.2008.12.009>
- Terhaar, J., Kwiatkowski, L., & Bopp, L. (2020). Emergent constraint on Arctic Ocean acidification in the twenty-first century. *Nature*, 582, 379–383. <https://doi.org/10.1038/s41586-020-2360-3>
- Tu, Z., Le, C., Bai, Y., Jiang, Z., Wu, Y., Ouyang, Z., et al. (2021). Increase in CO₂ uptake capacity in the Arctic Chukchi Sea during summer revealed by satellite-based estimation. *Geophysical Research Letters*, 48(15). <https://doi.org/10.1029/2021GL093844>
- Wakita, M., Sasaki, K., Nagano, A., Abe, H., Tanaka, T., Nagano, K., et al. (2021). Rapid Reduction of pH and CaCO₃ saturation state in the tsugaru strait by the intensified tsugaru warm current during 2012–2019. *Geophysical Research Letters*, 48(10). <https://doi.org/10.1029/2020GL091332>
- Wang, M., & Overland, J. E. (2009). A sea ice free summer Arctic within 30 years? *Geophysical Research Letters*, 36(7), 550–556. <https://doi.org/10.1029/2009GL037820>
- Wanninkhof, R. (2014). Relationship between wind speed and gas exchange over the ocean revisited. *Limnology and Oceanography: Methods*, 12(6), 351–362. <https://doi.org/10.4319/lom.2014.12.351>

- Weiss, R. F. (1974). Carbon dioxide in water and seawater: The solubility of a non-ideal gas. *Marine Chemistry*, 2(3), 203–215. [https://doi.org/10.1016/0304-4203\(74\)90015-2](https://doi.org/10.1016/0304-4203(74)90015-2)
- Woodgate, R. A., & Rebec Ca, A. (2017). Increases in the Pacific inflow to the Arctic from 1990 to 2015, and insights into seasonal trends and driving mechanisms from year-round Bering Strait mooring data. *Progress in Oceanography*, 160, 124–154. <https://doi.org/10.1016/j.pocean.2017.12.007>
- Woodgate, R. A., Weingartner, T. J., & Lindsay, R. (2012). Observed increases in Bering Strait oceanic fluxes from the Pacific to the Arctic from 2001 to 2011 and their impacts on the Arctic Ocean water column. *Geophysical Research Letters*, 39(24). <https://doi.org/10.1029/2012gl054092>
- Woosley, R. J., Millero, F. J., & Wanninkhof, R. (2016). Rapid anthropogenic changes in CO₂ and pH in the Atlantic ocean: 2003-2014. *Global Biogeochemical Cycles*, 30, 70–90. <https://doi.org/10.1002/2015GB005248>
- Wynn, J. G., Robbins, L. L., & Anderson, L. G. (2016). Processes of multibathyal aragonite undersaturation in the Arctic Ocean. *Journal of Geophysical Research*, 121(11), 8248–8267. <https://doi.org/10.1002/2016JC011696>
- Yamamoto-Kawai, M., McLaughlin, F. A., Carmack, E. C., Nishino, S., & Shimada, K. (2009). Aragonite undersaturation in the Arctic Ocean: Effects of Ocean acidification and sea ice melt. *Science*, 326(5956), 1098–1100. <https://doi.org/10.1126/science.1174190>
- Zheng, Z., Luo, X., Wei, H., Zhao, W., & Qi, D. (2021). Analysis of the seasonal and interannual variations of air-sea CO₂ flux in the Chukchi Sea using A coupled ocean-sea ice-biogeochemical model. *Journal of Geophysical Research: Oceans*, 126. <https://doi.org/10.1029/2021JC017550>